Photoionization of the $4d^{10}$ subshell of cadmium: Photoelectron angular distributions and polarization of fluorescence radiation

Constantine E. Theodosiou* and Anthony F. Starace†
Fakultät für Physik der Universität Freiburg, D-7800 Freiburg i.Br., Federal Republic of Germany

B. R. Tambe‡ and Steven T. Manson
Department of Physics and Astronomy, Georgia State University, Atlanta, Georgia 30303
(Received 3 October 1980)

Relativistic Dirac-Fock calculations are presented for the photoelectron angular distribution asymmetry parameter β corresponding to $4d$-subshell photoionization in Cd and for the linear polarization P_L of the subsequent fluorescence radiation, for photon energies less than 185 eV. Near threshold, our results for β lie lower than previous relativistic Dirac-Slater and nonrelativistic many-body-perturbation-theory (MBPT) calculations. The agreement with very recent measurements by Heinzmann and Schönhense is very good. Our calculations show that $P_L(^2D_{5/2}\rightarrow{}^2P_{3/2}) = -0.059$ and -0.058 at incident photon energies $h\nu = 40.2$ and 45.6 eV, respectively. These results lie above the nonrelativistic independent-electron theory absolute maximum of -0.061 for P_L, but the agreement with recent measurements lying above this maximum is still not very good. Except for this peaking of $P_L(^2D_{5/2}\rightarrow{}^2P_{3/2})$ above the nonrelativistic theory maximum for $40.2 \leq h\nu \leq 45.6$ eV, our results at other energies are in general agreement with the nonrelativistic MBPT calculations of Carter and Kelly. We also find that $P_L(^2D_{3/2}\rightarrow{}^2P_{3/2}) = +0.134$ at $h\nu = 21.2$ eV, in excellent agreement with the experimental value of $+0.12\pm0.04$ of Caldwell and Zare.

I. INTRODUCTION AND PERSPECTIVE

The photoionization of the cadium $4d$ subshell is interesting from the theoretical point of view because Cd is not a pure LS- or jj-coupling case and $4d$ is an *inner* subshell. Experimentally, one can measure the photoionization cross section σ, and the photoelectron angular distributions β, of the process

$$\mathrm{Cd}(4d^{10}5s^{2}\,{}^1S) + \gamma \rightarrow \mathrm{Cd}^+(4d^9 5s^2\,{}^2D_{5/2,3/2}) + \epsilon l, \quad l = 1, 3 \qquad (1)$$

or the linear polarization P_L, of the emitted fluorescence light from the transitions

$$\mathrm{Cd}^+(4d^9 5s^2\,{}^2D_{5/2}) \rightarrow \mathrm{Cd}^+(4d^{10}5p\,{}^2P_{3/2}) + \gamma', \qquad (2)$$

$$\mathrm{Cd}^+(4d^9 5s^2\,{}^2D_{3/2}) \rightarrow \mathrm{Cd}^+(4d^{10}5p\,{}^2P_{3/2,1/2}) + \gamma'', \qquad (3)$$

following the photoionization. The parameters β and P_L provide more detailed information about the photoionization process than σ, because they depend more critically on the ion core state and the interactions between the escaping photoelectron and the ion.

The $4d$-photoionization cross section has been the subject of several experimental[1-3] and theoretical[4-7] investigations during the last decade, and the agreement between theory and experiment has reached a satisfactory level.[7] This, however, has not been the case for either the photoelectron angular-distribution asymmetry parameter or the linear polarization of the emitted fluorescence light.

Harrison[8] has obtained β at $h\nu = 21.2$ eV, the He I line, by measuring the photoelectron angular distribution. The Dirac-Slater (DS) calculations of Walker and Waber[5] (in pure jj coupling) and the Hartree-Fock (HF) many-body-perturbation-theory (MBPT) treatment of Carter and Kelly[6] (in pure LS coupling) disagree completely with Harrison's values. In an effort to resolve this discrepancy, the Dill-Fano[9] angular-momentum transfer theory for β was applied[10] to examine the effects of anisotropic interactions between the ion core and the photoelectron as it escapes. The work was only analytical and one of its major results was that the anisotropic interactions result mainly in a reduction of the asymmetry parameters $\beta_{5/2}$ and $\beta_{3/2}$ [see Eqs. (4) and (5) below]. Heinzmann and Schönhense have very recently remeasured[11] $\beta_{5/2}$ and $\beta_{3/2}$ at $h\nu = 21.2$ eV finding completely different values from Harrison.[8] The new experimental points are in *qualitative* agreement with the DS and HF-MBPT calculations but lie lower than both of them.

Photoionization of an atom even with unpolarized incident radiation leads to an alignment of the resulting ion.[12,13] That is, the magnetic quantum states M_J of the ion have an unequal occupation probability distribution which may be detected by measurement of the polarization of the subsequent fluorescence radiation.[14-21] The polarization of the $^2D_{5/2}\rightarrow{}^2P_{3/2}$ and $^2D_{3/2}\rightarrow{}^2P_{3/2}$ transitions [(2) and (3) above] have been measured recently by Caldwell and Zare[15] using 21.2-eV incident radiation. Mauser and Mehlhorn[20] have also measured the polar-

ization of the $^2D_{5/2} \rightarrow {}^2P_{3/2}$ fluorescence transition using a mixture of 21.2 (HeI) and 40.8 eV (HeII) as well as 26.9 eV (NeII) incident radiation. Nonrelativistic theoretical calculations[16,22] of the polarization of fluorescence radiation for the $^2D_{5/2} \rightarrow {}^2P_{3/2}$ transition lie substantially lower than all three experimental measurements for this transition. In fact, Caldwell and Zare[15] have shown that in nonrelativistic independent-electron approximation the upper limit of the linear polarization lies below the experimentally measured values, indicating the importance of spin-orbit and other relativistic interaction effects. No theoretical calculations have yet been carried out for the $^2D_{3/2} \rightarrow {}^2P_{3/2}$ fluorescence transition.

In this paper relativistic Dirac-Fock (DF) results are presented for the photoelectron angular-distribution asymmetry parameters $\beta_{5/2}$ and $\beta_{3/2}$ and the polarization of the $^2D_{5/2} \rightarrow {}^2P_{3/2}$ and $^2D_{3/2} \rightarrow {}^2P_{3/2,1/2}$ fluorescence transitions subsequent to $4d^{10}$-subshell photoionization in Cd. Numerical details of the Dirac-Fock calculations have been given elsewhere.[7] The choice of the Dirac-Fock calculational scheme was made because we are interested specifically in the effects of the differing thresholds, $\Delta E(^2D_{3/2} - {}^2D_{5/2}) \simeq 0.7$ eV, which can only show up in a relativistic description; no nonrelativistic treatment can treat the Cd $4d$ photoionization accurately near threshold, since LS coupling, without the inclusion of spin-orbit and other relativistic interactions, cannot give different behavior for the two thresholds $^2D_{5/2}$ and $^2D_{3/2}$. Our Dirac-Fock calculation uses jj coupling which distinguishes between the two thresholds and in addition partially accounts for the photoelectron-ion-core anisotropic interactions. The jj-coupling scheme does not describe Cd^+ exactly either; however, the dissociation channels of the $e^- + Cd^+$ system, which are appropriate at large electron-ion separations, are labeled *exactly* by jj quantum numbers.[10] Therefore, we expect that our DF results presented below will be more realistic than any nonrelativistic calculation, even MBPT, *near the fine-structure thresholds*. They should also be more reliable than the relativistic central-potential (DS) calculation, because in the Dirac-Slater approach exchange effects between photoelectron and ion-core electrons, which are very important near threshold, are included only very approximately and their variation with energy is omitted entirely.

TABLE I. Photoionization amplitudes $S_l(j_t)$ for $Cd^+(^2D_{5/2})$ and $Cd^+(^2D_{3/2})$ in jj coupling.

$^2D_{5/2}$

$$S_p(2) = i\frac{\sqrt{2}}{5} R_{p3/2} \exp(i\phi_{p3/2})$$

$$S_f(2) = i(35\sqrt{3})^{-1}[R_{f5/2} \exp(i\phi_{f5/2}) + 20 R_{f7/2} \exp(i\phi_{f7/2})]$$

$$S_f(3) = i\frac{2}{7\sqrt{21}}[R_{f5/2} \exp(i\phi_{f5/2}) - R_{f7/2} \exp(i\phi_{f7/2})]$$

$^2D_{3/2}$

$$S_p(1) = i(3\sqrt{6})^{-1}[-R_{p1/2} \exp(i\phi_{p1/2}) + R_{p3/2} \exp(i\phi_{p3/2})]$$

$$S_p(2) = i(3\sqrt{2})^{-1}[R_{p1/2} \exp(i\phi_{p1/2}) + (\tfrac{1}{5}) R_{p3/2} \exp(i\phi_{p3/2})]$$

$$S_f(2) = -i\frac{\sqrt{3}}{5} R_{f5/2} \exp(i\phi_{f5/2})$$

II. PHOTOELECTRON ANGULAR DISTRIBUTIONS

Using the Dill-Fano approach[9] of treating anisotropic interactions between photoelectron and ion core, the photoelectron angular-distribution asymmetry parameters for the $^2D_{5/2}$ and $^2D_{3/2}$ states may be written[10]

$$\beta_{5/2} = \frac{4|S_f(2)|^2 + |S_p(2)|^2 - 6\sqrt{6}\,\mathrm{Re}[S_f(2)S_p^*(2)] - 7|S_f(3)|^2}{5[|S_f(2)|^2 + |S_p(2)|^2 + 7|S_f(3)|^2]}, \tag{4}$$

$$\beta_{3/2} = \frac{4|S_f(2)|^2 + |S_p(2)|^2 - 6\sqrt{6}\,\mathrm{Re}[S_f(2)S_p^*(2)] - 3|S_p(1)|^2}{5[|S_f(2)|^2 + |S_p(2)|^2 + 3|S_p(1)|^2]}. \tag{5}$$

Here $S_l^{J_c}(j_t)$ denotes the photoionization amplitude for a given angular-momentum transfer j_t, a photoelectron orbital angular momentum $l(=j_t, j_t \pm 1)$, and an ionic-core state with total angular momentum J_c. [The superscript J_c is dropped in Eqs. (4) and (5) as well as in the equations below for convenience.] The amplitudes $S_f(3)$ and $S_p(1)$ are nonzero due to effects of the anisotropic interactions and tend to decrease the values of $\beta_{5/2,3/2}$ obtained in their absence. The explicit form of the amplitudes $S_l(j_t)$ depends on the approximation and angular-momentum coupling considered and is given for the general case in Ref. 10. In our specific case we use pure jj coupling and Table I gives the appropriate $S_l(j_t)$ expressions, in terms of the radial matrix elements R_{lj}. These matrix elements involve radial integrals defined in terms of the large and small components of the radial wave functions and their form is given elsewhere.[23] Using these expressions in Eqs. (4) and (5) we have

TABLE II. Photoelectron angular-distribution asymmetry parameter $\beta_{5/2}$ and linear fluorescence polarization $P_L(^2D_{5/2} \rightarrow {}^2P_{3/2})$ corresponding to $Cd^+(^2D_{5/2})$.

Photoelectron energy ϵ (eV)	Photon energy $h\nu$ (eV)	$\beta_{5/2}$	$P_L(^2D_{5/2} \rightarrow {}^2P_{3/2})$
1.1	18.65	0.950	−0.176
2.2	19.74	0.499	−0.156
3.5	21.09	0.104	−0.133
6.2	23.81	−0.281	−0.104
7.6	25.17	−0.345	−0.095
10.3	27.89	−0.363	−0.082
11.7	29.25	−0.342	−0.077
13.0	30.61	−0.312	−0.073
17.1	34.70	−0.198	−0.065
22.6	40.14	0.039	−0.059
28.0	45.58	0.108	−0.058
41.6	59.18	0.427	−0.063
55.2	72.79	0.716	−0.071
68.8	86.39	1.008	−0.077
82.4	100.00	1.325	−0.083
109.6	127.21	1.941	−0.129
136.8	154.42	−0.404	−0.202
164.1	181.63	−0.383	−0.115

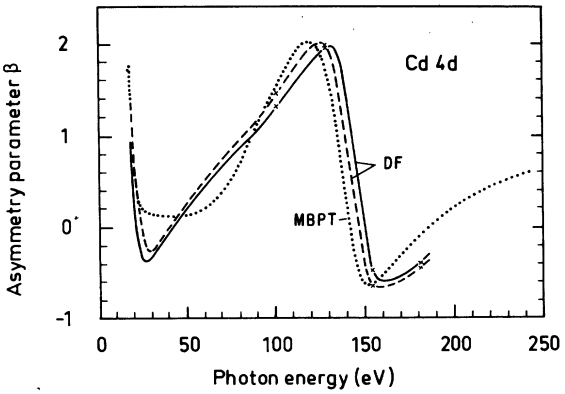

FIG. 1. Photoelectron angular-distribution asymmetry parameters $\beta_{5/2}$ and $\beta_{3/2}$ for the cadmium $4d$ subshell plotted vs photon energy (eV). Theory: $4d_{5/2}$ solid line, $4d_{3/2}$ dashed line, is the present Dirac-Fock calculation (here and in Fig. 3 the x's at higher energies represent the actually calculated values and the line through them is drawn freehand. At low energies the calculated points are dense enough to be represented by the curves exactly). Dotted line represents the nonrelativistic many-body-perturbation-theory calculation of Carter and Kelly (Ref. 6).

$$\beta_{5/2} = [98R^2_{p3/2} - 32R^2_{f5/2} + 500R^2_{f7/2} + 120R_{f5/2}R_{f7/2}\cos(\phi_{f5/2} - \phi_{f7/2}) - 84R_{p3/2}R_{f5/2}\cos(\phi_{p3/2} - \phi_{f5/2}) - 1680R_{p3/2}R_{f7/2}\cos(\phi_{p3/2} - \phi_{f7/2})] \times [35(14R^2_{p3/2} + R^2_{f5/2} + 20R^2_{f7/2})]^{-1}, \quad (6)$$

$$\beta_{3/2} = [-4R^2_{p3/2} + 36R^2_{f5/2} + 10R_{p1/2}R_{p3/2}\cos(\phi_{p1/2} - \phi_{p3/2}) - 18R_{p3/2}R_{f5/2}\cos(\phi_{p3/2} - \phi_{f5/2}) - 90R_{p1/2}R_{f5/2}\cos(\phi_{p1/2} - \phi_{f5/2})] \times [5(5R^2_{p1/2} + R^2_{p3/2} + 9R^2_{f5/2})]^{-1}, \quad (7)$$

with $\phi_{lj} = \delta_{\epsilon lj} + \xi_{\epsilon lj}$, where $\delta_{\epsilon lj}$ is the short-range phase shift and $\xi_{\epsilon lj}$ is the relativistic Coulomb phase shift which reduces to $\arg\Gamma(l+1-i/\sqrt{\epsilon})$ in the nonrelativistic limit.[23] Both Eqs. (6) and (7) reduce to the Cooper-Zare expression[24]

$$\beta_{CZ} = [2R_p^2 + 12R_f^2 - 36R_pR_f\cos(\phi_f - \phi_p)]/[5(R_p^2 + 3R_f^2)] \quad (8)$$

in the nonrelativistic limit (i.e., $R_{f5/2} = R_{f7/2} = R_f$, $R_{p1/2} = R_{p3/2} = R_p$, $\phi_{f5/2} = \phi_{f7/2} = \phi_f$, and $\phi_{p1/2} = \phi_{p3/2} = \phi_p$).

Our Dirac-Fock results for $\beta_{5/2}$ and $\beta_{3/2}$ are given in Table II for a wide range of photon energies. They are compared in Fig. 1 with the nonrelativistic MBPT values of Carter and Kelly. We note that the two calculations have quite different behavior for $h\nu = 20$–80 eV, whereas they agree reasonably well below and above that energy region. Considering that the DF and HF-MBPT results for the total photoionization cross section are in fair agreement with each other in shape

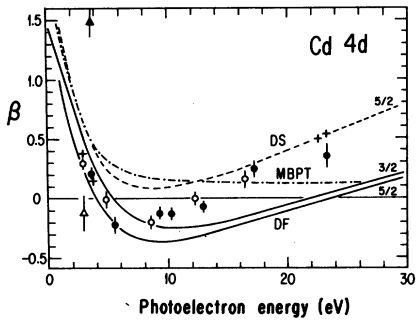

FIG. 2. Expansion of the low photoelectron energy part of Fig. 1. Experiment (open symbols for $\beta_{3/2}$; full symbols for $\beta_{5/2}$): ◇, ◆, Schönhense [Ref. 11(b)]; △, ▲, Harrison (Ref. 8). Theory: DF represents present Dirac-Fock results; DS represents Dirac-Slater calculation of Walker and Waber (Ref. 6) (the result for $\beta_{3/2}$ is almost identical to the $\beta_{5/2}$ shown here, due to the Slater approximation being used for the exchange potential); MBPT represents the many-body perturbation theory of Carter and Kelly (Ref. 6); + represents the ground-state-inversion-potential method by Suzer *et al.* (Ref. 25).

and magnitude,[7] the discrepancy in this case should be attributed to the different partial-wave phase shifts, which play a critical role for β's. The Dirac-Slater calculation of Walker and Waber[5] produces curves similar to ours but higher in magnitude and never reaching negative values. We show in Fig. 2 an expanded version of Fig. 1 at low energies for easier comparison with experiment. Harrison's values[8] are quite far off and inverted in magnitude compared to theory. The most recent measurements by Schönhense[11(b)] are seen to agree very well, except for the smaller $D_{5/2}-D_{3/2}$ splitting, with our calculation below photoelectron energies ~8 eV. At higher energies however, they lie higher than our curves and, specifically, halfway between the DF and DS[5] results. We also show four theoretical values due to Süzer *et al.*, who used a ground-state inversion-potential method.[25] It seems probable[11,25] that Harrison[8] has fitted an inappropriate photoelectron angular-distribution formula to obtain the asymmetry parameters $\beta_{5/2}$ and $\beta_{3/2}$.

III. POLARIZATION OF THE Cd $4d^{10}$ FLUORESCENCE RADIATION

A. Cd($^2D_{5/2}$) state

The linear polarization of the $^2D_{5/2}\rightarrow{}^2P_{3/2}$ fluorescence radiation in Cd measured at 90° to the incident unpolarized radiation beam may be written[18,19]

$$P_L(^2D_{5/2}\rightarrow{}^2P_{3/2})=\frac{-\frac{7}{2}|S_p(2)|^2-|S_f(2)|^2+\frac{21}{4}|S_f(3)|^2+\sqrt{7}\,\mathrm{Re}[S_f(2)S_f^*(3)]}{\frac{31}{2}|S_p(2)|^2+\frac{49}{3}|S_f(2)|^2+\frac{301}{12}|S_f(3)|^2+\frac{1}{3}\sqrt{7}\,\mathrm{Re}[S_f(2)S_f^*(3)]}. \quad (9)$$

Using the expressions for the photoionization amplitudes $S_l(j_t)$ given in Table I we find the following expression for $P_L(^2D_{5/2}\rightarrow{}^2P_{3/2})$ in terms of the relativistic radial dipole matrix elements R_{lj}:

$$P_L(^2D_{5/2}\rightarrow{}^2P_{3/2})=\frac{-49R^2_{p3/2}+4R^2_{f5/2}-25R^2_{f7/2}}{217R^2_{p3/2}+18R^2_{f5/2}+325R^2_{f7/2}}. \quad (10)$$

Equation (10) reduces to the following result of Caldwell and Zare[15] in the nonrelativistic limit (i.e., $R_{f5/2}=R_{f7/2}=R_f$ and $R_{p3/2}=R_{p1/2}=R_p$):

$$P_L^{\mathrm{NR}}(^2D_{5/2}\rightarrow{}^2P_{3/2})=\frac{-7R_p^2-3R_f^2}{31R_p^2+49R_f^2}. \quad (11)$$

Note that $P_L^{\mathrm{NR}}(^2D_{5/2}\rightarrow P_{3/2})$ has a maximum value of -0.0612 when $R_p=0$ and a minimum value of -0.2258 when $R_f=0$. In contrast, Klar[18] has examined the exact Eq. (9) for $P_L(^2D_{5/2}\rightarrow{}^2P_{3/2})$ and has found that it is bounded between the values -0.226 and $+0.209$.

Our Dirac-Fock results for $P_L(^2D_{5/2}\rightarrow{}^2P_{3/2})$ are given in Table II. We note that at the two incident photon energies 40.2 and 45.6 eV our results for $P_L(^2D_{5/2}\rightarrow{}^2P_{3/2})$ lie above the nonrelativistic upper limit of -0.0612. As shown in Fig. 3, however, even with this excursion of our calculated $P_L(^2D_{5/2}\rightarrow{}^2P_{3/2})$ above the nonrelativistic independent-electron theory maximum, our results still lie below the measured values[15,20] above the nonrelativistic maximum. It is quite likely that electron-correlation effects such as interchannel coupling might shift the position of our maximum to lower energies or raise our entire curve. Also as shown in Fig. 3, our Dirac-Fock results agree very well with the nonrelativistic MBPT calculations of Carter and Kelly[6,22] and with the nonrelativistic Hermann-Skillman model[26] (HS) calculations of Berezhko *et al.*[16] in the region near threshold where $P_L(^2D_{5/2}\rightarrow{}^2P_{3/2})$ rises rapidly. The nonrelativistic results then attain a plateau while our

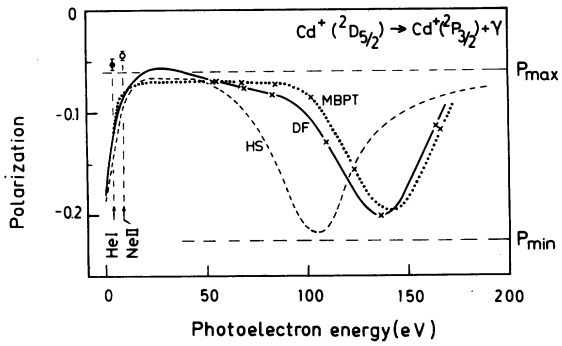

FIG. 3. Linear polarization P_L for the fluorescence transition $^2D_{5/2}\rightarrow{}^2P_{3/2}$ of Cd$^+$ $4d^9(^2D_{5/2})$ plotted vs photoelectron energy (eV). ϕ, represents the experimental measurement of Caldwell and Zare (Ref. 15) using He I incident radiation; the experimental measurement of Mauser and Mehlhorn (Ref. 20) at this energy is identical on the scale of this figure. ϕ, represents the experimental measurement of Mauser and Mehlhorn (Ref. 20) using Ne II incident radiation. MBPT represents the many-body-perturbation-theory results (indicated by x's at high energy) of Carter and Kelly (Refs. 6 and 22). HS represents the Hermann-Skillman central-potential model calculations of Berezhko *et al.* (Ref. 16). DF represents the present Dirac-Fock results (indicated by x's at high energy). The horizontal dashed lines indicate the nonrelativistic theory limits $P_{\max}=-0.0612$ and $P_{\min}=-0.2258$ [cf. Eq. (12)].

relativistic values peak above the nonrelativistic maximum for $P_L(^2D_{5/2} \rightarrow {}^2P_{3/2})$. At higher incident photon energies our results disagree with the HS calculation but are in reasonable agreement with the MBPT calculation. All theoretical curves show a deep minimum above a photoelectron energy of 100 eV due to a sign change of the f-wave radial dipole matrix elements. This minimum corresponds to the Cooper minimum in the photoionization cross section[6,7,22] and to the high-energy minimum in the β parameter (of Sec. II).

B. Cd($^2D_{3/2}$) state

We are concerned here with two transitions: the $^2D_{3/2} \rightarrow {}^2P_{3/2}$ and the $^2D_{3/2} \rightarrow {}^2P_{1/2}$. Expressions for P_L for these transitions for measurements at 90° to the incident unpolarized radiation are[27]

$$P_L(^2D_{3/2} \rightarrow {}^2P_{3/2}) = \frac{-3|S_p(1)|^2 + 7|S_p(2)|^2 + 2|S_f(2)|^2 + 6\sqrt{3}\,\mathrm{Re}[S_p(1)S_p^*(2)]}{19|S_p(1)|^2 + (107/3)|S_p(2)|^2 + 34|S_f(2)|^2 + 2\sqrt{3}\,\mathrm{Re}[S_p(1)S_p^*(2)]}, \tag{12}$$

$$P_L(^2D_{3/2} \rightarrow {}^2P_{1/2}) = \frac{-7|S_p(2)|^2 + 3|S_p(1)|^2 - 2|S_f(2)|^2 - 6\sqrt{3}\,\mathrm{Re}[S_p(1)S_p^*(2)]}{(73/3)|S_p(2)|^2 + 17|S_p(1)|^2 + 26|S_f(2)|^2 - 2\sqrt{3}\,\mathrm{Re}[S_p(1)S_p^*(2)]}. \tag{13}$$

Using the expressions for the photoionization amplitudes $S_t(j_t)$ given in Table I we find that Eqs. (12) and (13) reduce to the following expressions in terms of the relativistic radial dipole matrix elements R_{ij}:

$$P_L(^2D_{3/2} \rightarrow {}^2P_{3/2}) = \frac{(\frac{25}{9})R_{p1/2}^2 - (\frac{4}{9})R_{p3/2}^2 + R_{f5/2}^2}{(\frac{275}{27})R_{p1/2}^2 + (\frac{46}{27})R_{p3/2}^2 + 17R_{f5/2}^2}, \tag{14a}$$

$$P_L(^2D_{3/2} \rightarrow {}^2P_{1/2}) = \frac{-(\frac{25}{9})R_{p1/2}^2 + (\frac{4}{9})R_{p3/2}^2 - R_{f5/2}^2}{(\frac{175}{27})R_{p1/2}^2 + (\frac{44}{27})R_{p3/2}^2 + 13R_{f5/2}^2}. \tag{14b}$$

In the nonrelativistic limit (i.e., $R_{p1/2} = R_{p3/2} = R_p$ and $R_{f5/2} = R_{f7/2} = R_f$), Eqs. (15a) and (15b) reduce to the results of Caldwell and Zare[15]:

$$P_L^{\mathrm{NR}}(^2D_{3/2} \rightarrow {}^2P_{3/2}) = \frac{(\frac{7}{3})R_p^2 + R_f^2}{(\frac{107}{9})R_p^2 + 17R_f^2}, \tag{15a}$$

$$P_L^{\mathrm{NR}}(^2D_{3/2} \rightarrow {}^2P_{1/2}) = \frac{-(\frac{7}{3})R_p^2 - R_f^2}{(\frac{73}{9})R_p^2 + 13R_f^2}. \tag{15b}$$

In the nonrelativistic limit Eqs. (15) show that the polarization for the $^2D_{3/2} \rightarrow {}^2P_{3/2}$ transition ($^2D_{3/2} \rightarrow {}^2P_{1/2}$ transition) has a maximum value +0.1963 (−0.0769) when $R_f = 0$ ($R_p = 0$) and a minimum value +0.0588 (−0.2877) when $R_p = 0$ ($R_f = 0$).

Our results for $P_L(^2D_{3/2} \rightarrow {}^2P_{3/2})$ and $P_L(^2D_{3/2} \rightarrow {}^2P_{1/2})$ are shown in Table III. At none of the

TABLE III. Photoelectron angular-distribution asymmetry parameter $\beta_{3/2}$ and linear fluorescence polarizations $P_L(^2D_{3/2} \rightarrow {}^2P_{3/2})$ and $P_L(^2D_{3/2} \rightarrow {}^2P_{1/2})$ corresponding to $Cd^+(^2D_{3/2})$.

Photoelectron energy ϵ (eV)	Photon energy $h\nu$ (eV)	$\beta_{3/2}$	$P_L(^2D_{3/2} \rightarrow {}^2P_{3/2})$	$P_L(^2D_{3/2} \rightarrow {}^2P_{1/2})$
0.272	18.552	1.3734	0.1718	−0.2465
1.361	19.641	1.0417	0.1550	−0.2192
2.721	21.001	0.5808	0.1359	−0.1891
5.442	23.722	−0.0055	0.1083	−0.1474
6.803	25.083	−0.1384	0.0994	−0.1342
9.524	27.804	−0.2465	0.0875	−0.1170
10.884	29.164	−0.2529	0.0835	−0.1113
12.245	30.525	−0.2422	0.0803	−0.1069
16.326	34.606	−0.1597	0.0741	−0.0980
21.769	40.048	−0.0111	0.0696	−0.0918
27.211	45.490	0.1397	0.0671	−0.0883
40.816	59.095	0.4859	0.0644	−0.0846
54.422	72.700	0.8021	0.0641	−0.0842
68.027	86.305	1.1209	0.0661	−0.0869
81.632	99.910	1.4691	0.0721	−0.0953
108.843	127.120	1.9626	0.1298	−0.1797
136.054	154.330	−0.6366	0.1777	−0.2562
163.265	181.540	−0.4445	0.1097	−0.1494

photon energies for which we have calculated P_L do our relativistic Dirac-Fock results lie outside the nonrelativistic upper and lower bounds. Linear interpolation of our results in Table III gives a value for $P_L(^2D_{3/2} \rightarrow {}^2P_{3/2})$ of +0.134 at $h\nu = 21.2$ eV. In contrast to the case of $P_L(^2D_{5/2} \rightarrow {}^2P_{3/2})$, this result is in excellent agreement with the experimentally measured value[15] of $+0.12 \pm 0.04$ at this energy.

IV. DISCUSSION AND CONCLUSIONS

In this work, we have presented calculated results within the single-configuration Dirac-Fock approximation for the photoelectron angular-distribution asymmetry parameters and the fluorescence light polarizations corresponding to the $4d^{10}$-subshell photoionization process in cadmium.

Our results for $\beta_{5/2}$ and $\beta_{3/2}$ lie lower than the Dirac-Slater values. The agreement with Hartree-Fock MBPT calculations[6] is reasonable above photon energies of ~80 eV, whereas they disagree in magnitude and shape at lower energies. Specifically, the pronounced plateau predicted by MBPT (Ref. 6) is absent in our calculations and in the recent experimental results. Finally, our values are in very good agreement near threshold with recent experimental data,[11(b)] but are systematically too low for photoelectron energies $\epsilon \cong 8-23$ eV.

In the case of the $Cd^+(^2D_{5/2} \rightarrow {}^2P_{3/2})$ fluorescence transition, our calculated linear polarization curve is generally similar to the MBPT result except for the peak around 42-eV photon energy where our values exceed the nonrelativistic absolute maximum. In contrast, the experimentally measured polarization exceeds this nonrelativistic theoretical limit near 22-eV photon energy. The probable origin of this discrepancy should be attributed to the use of pure *jj* coupling and a single-configuration approximation. This results, for example, (here as well as in the *LS* case) in the linear polarization P_L being *independent* of the partial-wave phases.

In the case of the $Cd^+(^2D_{3/2})$ decay ours is the first calculation, and agreement with experiment for the $^2D_{3/2} \rightarrow {}^2P_{3/2}$ fluorescence transition is excellent.

ACKNOWLEDGMENTS

The authors wish to thank Professor W. Mehlhorn for drawing their attention to this problem. C.E.T. and A.F.S. each gratefully acknowledge the support of the Alexander von Humboldt Stiftung in the form of a Research Fellowship. S.T.M. gratefully acknowledges the research support of the U. S. Army Research Office.

---

*Present address: Department of Physics and Atmospheric Science, Drexel University, Philadelphia, Pennsylvania 19104.

†Permanent address: Behlen Laboratory of Physics, The University of Nebraska, Lincoln, Nebraska 68588.

‡Present address: Department of Physics, Southern Technical Institute, Marietta, Georgia 30060.

[1]R. B. Cairns, H. Harrison, and R. I. Schoen, J. Chem. Phys. 51, 5440 (1969).

[2]G. V. Marr and J. M. Austin, Proc. R. Soc. London A310, 137 (1969).

[3]S. P. Shannon and K. Codling, J. Phys. B 11, 1193 (1978).

[4]E. J. McGuire, Phys. Rev. 175, 20 (1968).

[5]T. E. H. Walker and J. T. Waber, J. Phys. B 7, 674 (1974).

[6]S. L. Carter and H. P. Kelly, J. Phys. B 11, 2467 (1978).

[7]B. R. Tambe, W. Ong, and S. T. Manson, Phys. Rev. A 23, 799 (1981).

[8]H. Harrison, J. Chem. Phys. 52, 901 (1970).

[9]D. Dill and U. Fano, Phys. Rev. Lett. 29, 1203 (1972).

[10]C. E. Theodosiou, J. Phys. B 12, L673 (1979).

[11](a) U. Heinzmann and G. Schönhense, Verh. Dtsch. Phys. Ges. (VI) 15, 583 (1980) and private communication; (b) G. Schönhense, J. Phys. B 14, L187 (1981).

[12]S. Flügge, W. Mehlhorn, and V. Schmidt, Phys. Rev. Lett. 20, 7 (1972).

[13]V. L. Jacobs, J. Phys. B 5, 2257 (1972).

[14]U. Fano and J. H. Macek, Rev. Mod. Phys. 45, 553 (1973).

[15]C. D. Caldwell and R. N. Zare, Phys. Rev. A 16, 255 (1977).

[16]E. G. Berezhko, N. M. Kabachnik, and V. S. Rostovsky, J. Phys. B 11, 1749 (1978).

[17]K. Blum and H. Kleinpoppen, Phys. Rep. 52, 203 (1979).

[18]H. Klar, J. Phys. B 12, L409 (1979).

[19]H. Klar, J. Phys. B 13, 2037 (1980).

[20]W. Mauser and W. Mehlhorn, Extended Abstracts of the VI International Conference on Vacuum Ultraviolet Radiation Physics, Charlottesville, Virginia, 1980 (unpublished), II-7.

[21]A. F. Starace, report (unpublished).

[22]Results for $P_L(^2D_{5/2} \rightarrow {}^2P_{3/2})$ presented in Ref. 20, using matrix elements from Ref. 6.

[23]W. Ong and S. T. Manson, Phys. Rev. A 19, 688 (1979).

[24]J. Cooper and R. N. Zare, *Lectures in Theoretical Physics*, edited by S. Geltman, K. Mahanthappa, and W. Brittin (Gordon and Breach, New York, 1969), Vol. 11c, p. 317.

[25]S. Süzer, P. R. Hilton, N. S. Huch, and S. Nordholm, J. Electron Spectrosc. Relat. Phenom. 12, 357 (1977).

[26]F. Hermann and S. Skillman, *Atomic Structure Calculations* (Prentice-Hall, Englewood Cliffs, New Jersey,

1963).

[27] These results may be obtained by substituting in Eq. (24) of Klar (Ref. 19) the following formulas for the asymmetry coefficients $A_{20}(q = \pm 1)$:

$^2D_{3/2} \rightarrow {}^2P_{3/2}$:

$$A_{20}(q=\pm1) = (\tfrac{1}{5})(\tfrac{3}{2})^{1/2}\{-3|S_p(1)|^2 + 7|S_p(2)|^2 + 2|S_f(2)|^2 + 6\sqrt{3}\,\mathrm{Re}[S_p(1)S_p^*(2)]\},$$

$^2D_{3/2} \rightarrow {}^2P_{1/2}$:

$$A_{20}(q=\pm1) = -(\tfrac{1}{4})(\tfrac{3}{2})^{1/2}\{7|S_p(2)|^2 - 3|S_p(1)|^2 + 2|S_f(2)|^2 + 6\sqrt{3}\,\mathrm{Re}[S_p(1)S_p^*(2)]\}.$$

Note that Klar's expressions for these coefficients (see Ref. 19, p. 2048) are in error in the case of the $^2D_{3/2}$ transitions in Cd.